

Zh.B. Sagdoldina<sup>1</sup>, D.R. Baizhan<sup>2\*</sup>, B.K. Rakhadilov<sup>3</sup>, D.B. Buitkenov<sup>4</sup>, N.E. Berdimuratov<sup>5</sup>,  
M.S. Zhaparova<sup>6</sup>

<sup>1,2,4,5,6</sup>Sarsen Amanzholov East Kazakhstan University, 30 Gvardeiskoi Divisii St. 34, 070020, Ust-Kamenogorsk, Kazakhstan;

<sup>1,2</sup>Shakarim University, Glinka St. 20 "a", 071412, Kazakhstan;

<sup>3</sup>Plasma Science LLP, 37 Serikbaev St., 070010, Kazakhstan

(\*E-mail: daryn.baizhan@mail.ru)

## Microstructure and mechanical properties of HA/Ti composite coatings applied by detonation spraying

This work presents the results of experimental studies of the structure and mechano-tribological properties of composite coatings based on hydroxyapatite (HA) and titanium in different ratios (wt. %): 30HA-70Ti, 50HA-50Ti, 70HA-30Ti. Composite coatings with a thickness of 40-50  $\mu\text{m}$  were applied to a substrate made of Grade 2 titanium by detonation spraying. Microstructures and phase compositions of as-sprayed coatings were analyzed by scanning electron microscopy and X-ray diffraction. The deposition mechanism of HA-Ti composite coatings was also examined. The results of the study showed that during detonation powder spraying from a mixture of HA-Ti, porous coatings are formed, consisting of the phases of hydroxyapatite  $\text{Ca}_{10}(\text{PO}_4)_6(\text{OH})_2$ , tricalcium phosphate, titanium, and titanium oxide. It was found that with a decrease in the content of hydroxyapatite in the composite, there is a decrease in the relative content of B-type carbonate ions in the structure, as well as a decrease in the content of the mineral phase as a whole. Composite coating 30HA-70Ti wt. % is the closest in structure to stoichiometric crystalline HA ( $\text{Ca/P} = 1.67$ ). At ratios of coatings 50HA-50Ti wt. %, an increase by 1.5-2 times in wear resistance is observed.

*Keywords:* hydroxyapatite, titanium, detonation spraying, coating, microstructures and phase composition, mechanical properties.

### Introduction

With the development of new concepts in the technology, production and application of implants for the bioengineering of bone tissue, the requirements for the functional, strength and aesthetic parameters of orthopedic structures have increased significantly [1]. First, this refers to the task of creating biocoatings, which are close to the structure of human bone tissue [2]. In order to stimulate the structure of natural bone, in recent years, the synthesis of hydroxyapatite  $\text{Ca}_{10}(\text{PO}_4)_6(\text{OH})_2$  has attracted considerable attention [3, 4]. Bioactive coatings based on hydroxyapatite and calcium phosphates are promising due to their biocompatibility and compositional proximity to bone tissue [5]. Hydroxyapatite (HA) provides ideal biocompatibility by actively stimulating osteogenesis and bone regeneration. However, HA coatings exhibit poor tribological properties, such as a strong tendency to adhesion, high and unstable coefficients of friction, and low resistance to wear during fretting. Therefore, it is also interesting to modify and progress the properties of the HA coating by including a metal in it [6]. HA/metal composite coatings are characterized by high mechanical and tribological properties [7]. Detonation technologies can be used to obtain HA/metal composite coatings [8]. The detonation gas spraying method has good prospects for the use in medicine, primarily due to the identity of the phase composition of the initial material and the formed coating. In this regard, the aim of this research is to study the effect of the ratio of the components on the structural-phase states, hardness and wear resistance of HA/metal composite coatings obtained by detonation spraying.

### Experimental

To obtain coatings, CCDS2000 detonation complex was used, having a system of electromagnetic gas valves that regulate the supply of fuel and oxygen, and control the purging of the system (Fig. 1). An acetylene-oxygen mixture, which is the most demanded fuel for detonation spraying of powder materials, was used as a fuel gas. The deposition was carried out at the  $\text{O}_2/\text{C}_2\text{H}_2$  ratio of 1.856. The volume of filling the barrel with a mixture is of acetylene-oxygen 50 %. Nitrogen was used as a carrier gas. The distance between the treated surface of the sample and the detonation barrel was 70 mm; the diameter of the straight barrel was 20 mm [9]. Commercially pure Grade 2 titanium (99.5 %) was used as a substrate. Before spraying, Grade 2 plates with dimensions of 30×30×3 mm were ground and polished, after which they were subjected to sand-

blasting. Sandblasting was carried out on the detonation unit using corundum powders with grain sizes of 0.5-1.3 mm with a volume of filling the barrel with an acetylene-oxygen mixture of 30 %. For spraying coatings, a mixture of titanium powders (grain size 10-12 microns) and HA (grain size 0.5-0.6 microns) were used in the ratios of 30/70, 50/50 and 70/30 (wt. %). Mechanical activation treatment was used to obtain a composite powder consisting of HA-Ti [10]. Mechanical activation of HA-Ti mixtures was carried out in a planetary ball mill PULVERISETTE 6 at a frequency of 380 rpm. The mechanical activation time was 60 s.

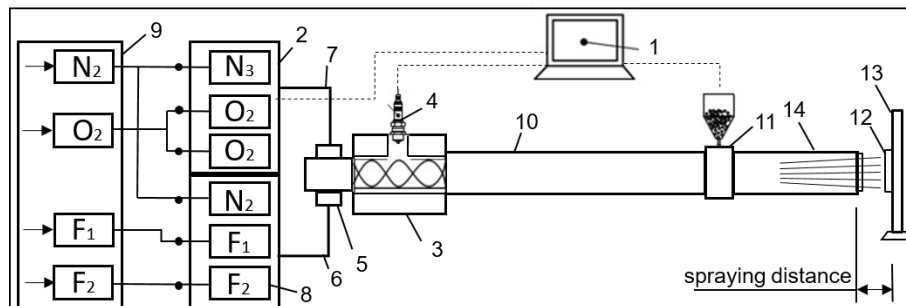


Figure 1. Scheme of the detonation complex CCDS2000: 1 — control computer, 2 — gas distributor, 3 — mixing-ignition chamber, 4 — spark plug, 5 — barrel valve, 6 — fuel line, 7 — oxygen line, 8 — gas valves, 9 — gas supply unit, 10 — part of the trunk, 11 — powder dispenser, 12 — sample; 13 — manipulator, 14 — muzzle.

The study of surface morphology was carried out by scanning electron microscopy (SEM) using backscattered electrons (BSE) on JSM-6390LV scanning electron microscope. The structure of the obtained samples was studied using Raman spectroscopy on AFM-Raman Solver Spectrum, NT-MDT spectrometer. To excite vibrational modes, a blue laser with a wavelength of 473 nm and a maximum laser power of 35 mW was used with a  $\times 100$  objective with a spot size of  $2 \cdot 10^{-6}$  m. The obtained spectra were processed by the Savitsky-Golay method [11] using a second-order polynomial. The error in recording the spectra was  $4 \text{ cm}^{-1}$ . The phase composition of the samples was studied by X-ray diffraction analysis on X'PertPro diffractometer using  $\text{CuK}\alpha$ -radiation. The study was carried out in the following modes: voltage across the tube was  $U = 40$  kV; tube current was  $I = 30$  mA; exposure time was 1 s; shooting step was  $0.02^\circ$ . The measurement of the tribological characteristics of the coatings was carried out in the sliding friction mode according to the “ball-disk” scheme on Anton Paar TRB3 tribometer. The sample rotation speed was 2 cm/s, the load was 5 N; a ball made of 100Cr6 steel with a diameter of 6 mm was used as a counterbody. Nanoindentation was carried out on NanoScan-4D nanohardness meter. In accordance with GOST R 8.748-2011. Using the Berkovich indenter, 10 injections were made at a load of 100 mN. Young's modulus and hardness were determined by the method of Oliver and Pharr [12].

### Results and Discussion

Figures 2-4 show diffraction patterns of the composite powder in different ratios of 30HA-70Ti, 50HA-50Ti, 70HA-30Ti (wt. %) and coatings obtained by detonation spraying. X-ray phase analysis showed that composite HA/Ti powder consists of two phases: HA and titanium. The diffractogram of composite 50HA/50Ti, 70HA/30Ti (wt. %) coatings (Fig. 3-4) is characterized by the appearance of peaks of the  $\alpha$ - $\text{Ca}_3(\text{PO}_4)_2$  (tricalcium phosphate) phase, while the main phase component of the coating retains the HA phase  $[\text{Ca}_{10}(\text{PO}_4)_6(\text{OH})_2]$ . However, in the diffraction pattern of coatings (Fig. 2b) with a powder composition of 30HA/70Ti the phase of tricalcium phosphate ( $\alpha$ - $\text{Ca}_3(\text{PO}_4)_2$ ) was not detected.  $\text{Ca}_3(\text{PO}_4)_2$  has a narrow mechanical strength compared to cortical bone, which limits its use in areas subject to low mechanical stress. However, when interacting with the environment, the body is completely replaced by biological tissues [13]. In addition, after detonation spraying of composite 50HA-50Ti and 70HA-30Ti coatings, intense phases of titanium oxide TiO were found (Fig. 3b, Fig. 4b). Titanium oxide is not considered a disadvantage in the biocompatibility of the implant, while the growth of the titanium oxide layer can improve adhesion to the bone tissue [14, 15]. The change in the phase composition of calcium phosphate coatings during detonation spraying is explained by high reactivity of titanium with respect to any substances at high temperatures [16].

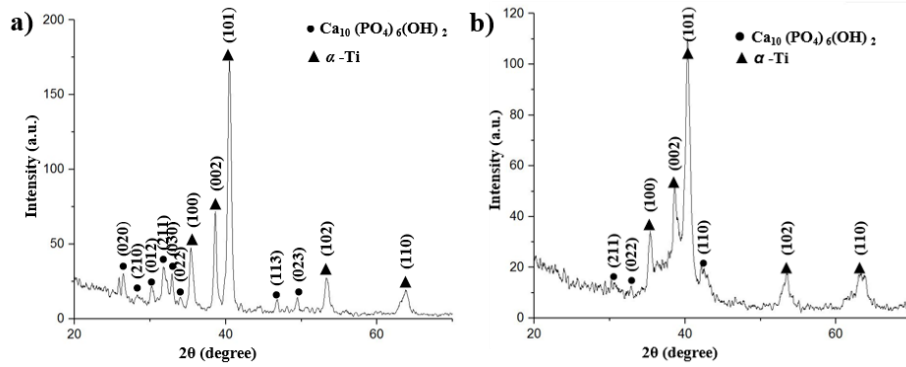


Figure 2. Diffraction patterns of the composite powder (a) and coating of 30HA-70Ti (wt. %), obtained by detonation spraying (b).

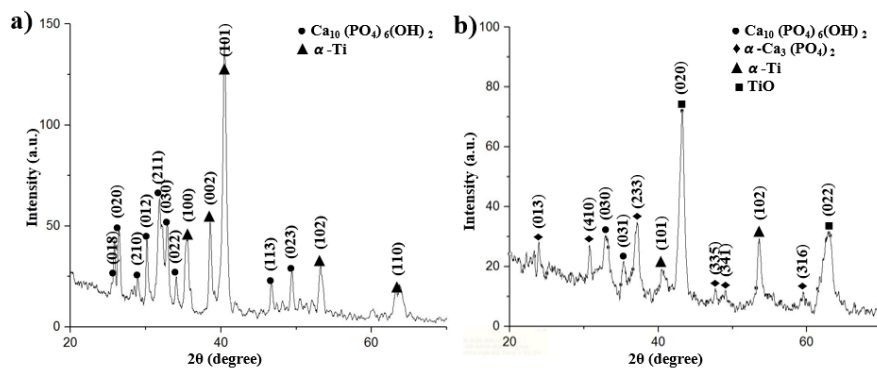


Figure 3. Diffraction patterns of composite powder (a) and coating of 50HA-50Ti (wt. %), obtained by detonation spraying (b).

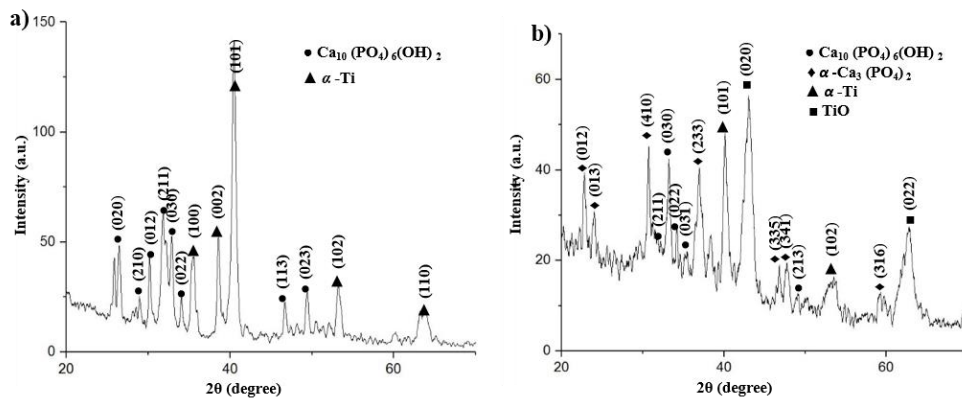


Figure 4. Diffraction patterns of (a) composite powder and coating of 70HA-30Ti (wt. %) obtained by detonation spraying (b).

To assess the microstructure of the surface of the composite coatings, the samples were analyzed by SEM. Figure 5 a-c shows SEM images and elemental analysis of composite 30HA-70Ti, 50HA-50Ti, 70HA-30Ti (wt. %) coatings. The morphology of the composite coatings (Fig. 5) showed the formation of a layered porous structure, which, in turn, promotes the effective growth of bone tissue into the pores of the implant. In the obtained coatings, pores are observed, which are formed when the coating particles melt. The formation of a porous structure and a pronounced relief is a feature of detonation technology, which can contribute to the widespread use of detonation coatings in medical implants.

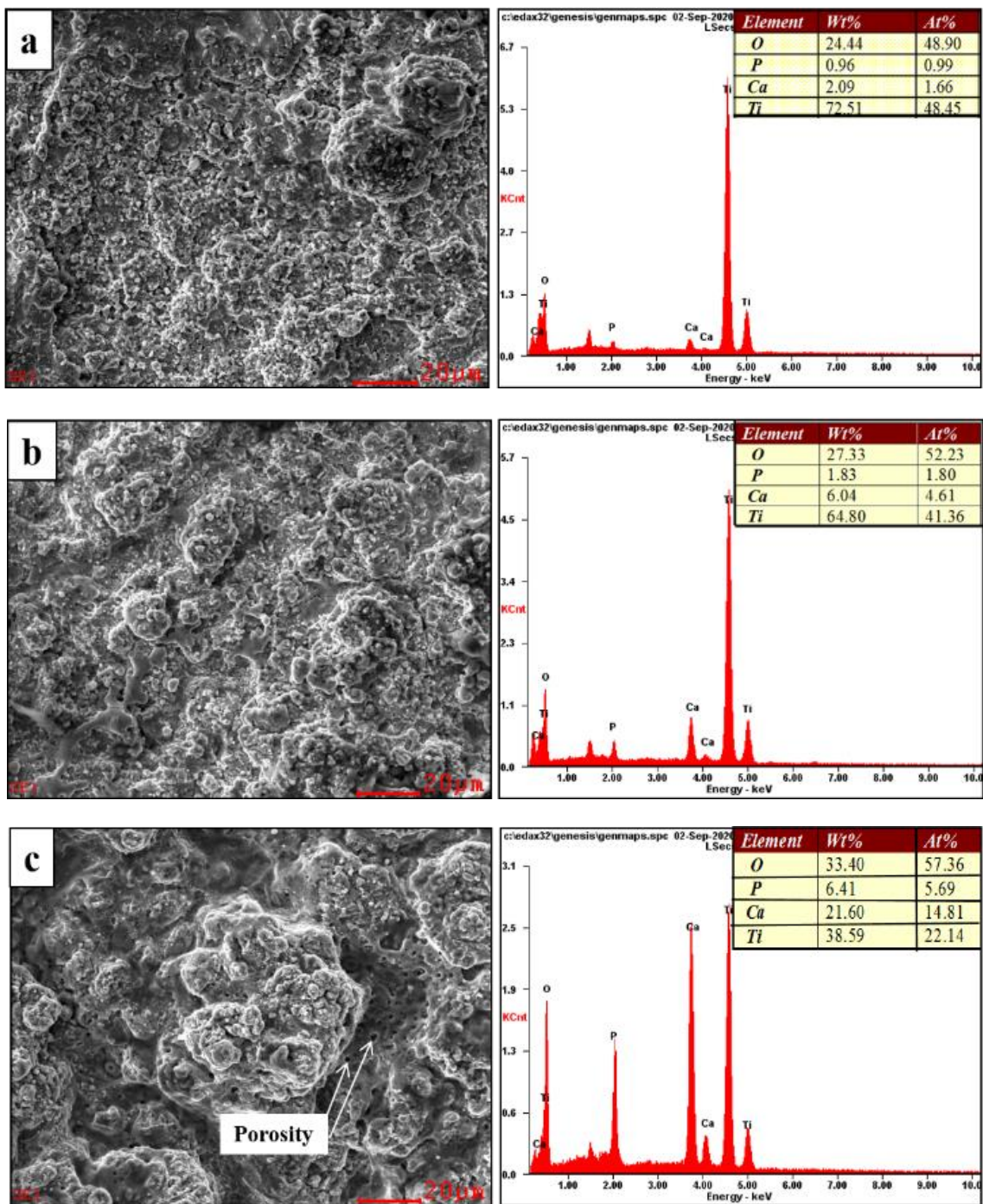


Figure 5. SEM image and EDS analysis of composite coatings (wt. %): 30HA-70Ti (a), 50HA-50Ti (b), 70HA-30Ti (c).

Figure 5 also shows the energy dispersive X-ray spectra of the coatings. Analysis of the elemental composition did not reveal the presence of other elements, except for the basic composition of the substrate and composite powder. According to the obtained results of the elemental analysis of composite coatings, it can be argued that detonation spraying does not cause a change in the chemical composition of the coating, and this factor is of decisive importance for the biocompatibility and preservation of the service life of the coating. The Ca/P ratio in coatings is one of the main parameters determining bioactivity. Elemental analysis allows comparing the concentrations of elements that make up composite coatings and calculate the Ca/P ratio. The atomic ratio of Ca/P in composite coatings ranges from 1.67-2.6. Table 1 shows the Ca/P atomic ratio for each group of composite coatings with a different content of hydroxyapatite. The atomic Ca/P ratio in composite coatings (30HA-70Ti) is 1.67; this result proves the possibility of obtaining a bioactive composition by detonation spraying.

Table 1.

**Atomic Ca/P ratio in composite coatings with different content of hydroxyapatite (wt. %):**

Coatings	Ca/P
30HA-70Ti	1.67
50HA-50Ti	2.56
70HA-30Ti	2.60

Figure 6 shows the Raman spectra of composite 30HA-70Ti, 50HA-50Ti, 70HA-30Ti coatings obtained by detonation spraying. The most noticeable intense band observed at  $961\text{ cm}^{-1}$  for all groups indicates that HA is the main phase component of the coatings. This band belongs to the P-O symmetric extension mode ( $\nu_1$ ) of the  $\text{PO}_4$  group and is the most characteristic band of carbonized apatites. The sharpness of this band confirms the good crystallinity of the HA coating [17]. Similarly, the bands associated with the antisymmetric stretching mode ( $\nu_3$ ) of  $\text{PO}_4$  groups show a shift from  $1045\text{ cm}^{-1}$  to the shoulder at  $1033\text{ cm}^{-1}$  (Table 2) [18]. With a decrease in HA-substitution (Fig. 6 c), the main apatite band at  $961\text{ cm}^{-1}$  demonstrates a broadening and a decrease in intensity, which indicates a decrease in the crystallinity of the formed mineral phase. In addition, it should be emphasized that this change in the carbonate content in the coatings is closely related to associated with changes in the growth morphology and size of crystallites, which occur with a change in temperature — higher atomic disorder corresponding to smaller crystal sizes (on a nanometer scale), the lattice becomes more and more ordered with increasing temperature.

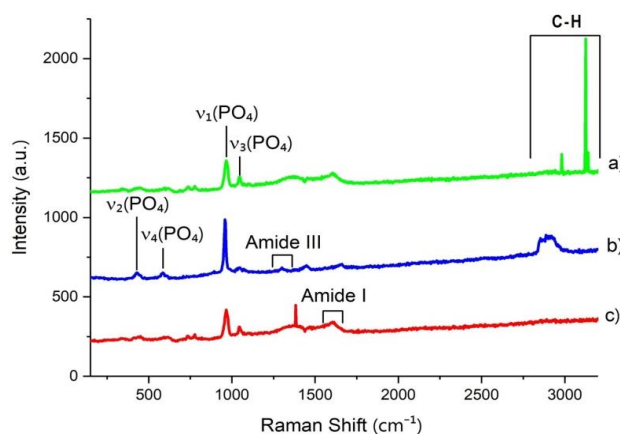


Figure 6. Raman spectra of composite coatings with different content of hydroxyapatite (wt. %): 70HA-30Ti (a); 50HA-50Ti (b); 30HA-70Ti (c).

The region of peaks at  $2880\text{--}3070\text{ cm}^{-1}$ , as a rule, is correlated with vibrations of C — H bonds ( $2880\text{--}2935$ ,  $3070\text{ cm}^{-1}$ ). Thus, according to the Raman spectroscopy data, the structural features of the composite coatings have been revealed with a decrease in the content of hydroxyapatite, a decrease in the relative content of B-type carbonate ions in the structure of hydroxyapatite is observed, as well as a decrease in the content of the mineral phase in general.

Table 2.

**Results with different frequencies of the corresponding lines**

Raman shift ( $\text{cm}^{-1}$ )	Assignment
423	$\text{PO}_4^{3-}$ $\nu_2$ (P-O deformation)
585	$\text{PO}_4^{3-}$ $\nu_4$ (P-O deformation)
950-965	$\text{PO}_4^{3-}$ $\nu_1$ (P-O deformation)
1030-1045	$\text{PO}_4^{3-}$ $\nu_3$ (P-O asymmetric valence)
1245-1270	Amide I II, C-N-H valence
1665-1675	Amide I, C-C-H valence
2880-2935, 3070	C-H vibrations

Hardness and elastic modulus are the main parameters determining the plasticity, an important characteristic of the material for practical application. Figure 7 shows the data on nanoindentation obtained on transverse thin sections of the coatings.

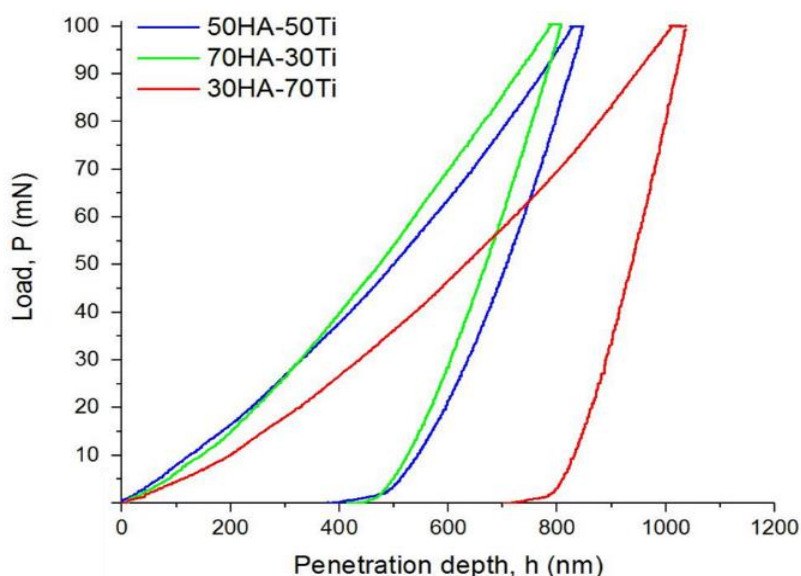


Figure 7. Curves of loading and unloading of composite coatings with different content of hydroxyapatite (wt. %).

To assess the resistance of a material to elastic deformation of fracture, the value of the ratio of hardness to Young's modulus  $H/E$ , also called the plasticity index of the material, was used [18]. In addition, to assess the mechanical properties of materials, the  $H^3/E^2$  parameter was used, which describes the resistance to plastic deformation [19]. It was found that the plasticity of the HA-Ti coating increases with an increase in the HA concentration. High values of  $H/E$  and  $H^3/E^2$  are indicators of high wear resistance, therefore, composite coatings with a composition of 70HA-30Ti, formed on Grade 2 titanium by detonation spraying, exhibit high performance properties of abrasive wear. The values of hardness, modulus of elasticity, elastic deformation of destruction ( $H/E$ ) and resistance to plastic deformation ( $H^3/E^2$ ) of composite coatings are given in Table 3.

Table 3.

**Hardness and elasticity modulus of composite coatings with different content of hydroxyapatite**

Sample	H, GPa	E, GPa	H/E	$H^3/E^2$
30HA-70Ti	$4.65 \pm 0.8$	$154.4 \pm 7$	0.03	$4.22 \cdot 10^{-3}$
50HA-50Ti	$7.5 \pm 0.9$	$129.3 \pm 8.8$	0.05	$25.23 \cdot 10^{-3}$
70HA-30Ti	$8.3 \pm 1.1$	$135.5 \pm 5.5$	0.06	$31.14 \cdot 10^{-3}$

Figure 8 shows micrographs of the surface and the results of measuring the roughness of composite coatings with different contents of hydroxyapatite (wt. %): 30HA-70Ti; 50HA-50Ti; 70HA-30Ti. The surface of all coatings has a heterogeneous structure with pores, typical layered, wavy arrangement of structural components. The surface roughness of the composite coatings was measured by the Ra parameter using a profilometer 130 on a 7 mm section on the sample surface. From the data obtained, the roughness of the composite coatings varies from 5.79 to 8.61  $\mu\text{m}$  with a change in the HA in the composite. Comparison of these dependences allows concluding that coatings obtained at low concentrations of HA in the composite have reduced values of the roughness parameter Ra, and as the concentration of HA in the composite increases, the roughness of the coatings increases. Composite coatings obtained by detonation spraying have a developed surface, which will serve as their improved fusion with bone tissue.

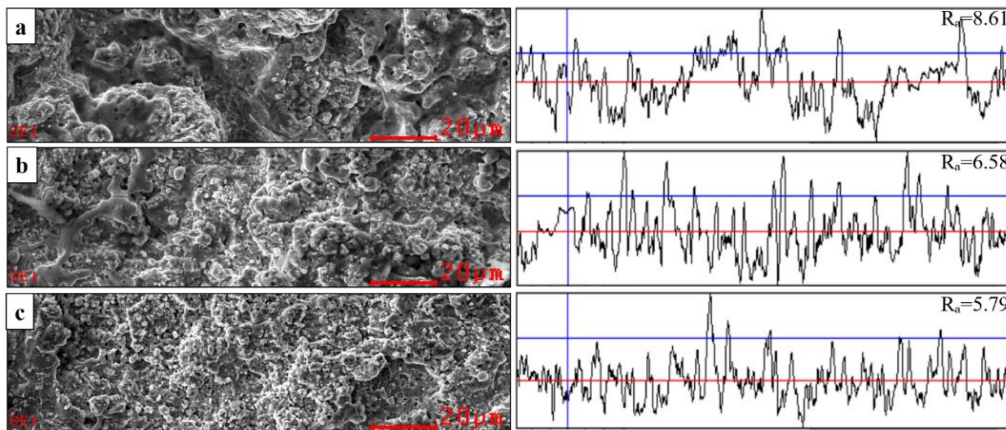


Figure 8 Micrographs and roughness of composite coatings with different content of hydroxyapatite (wt. %): 70HA-30Ti (a); 50HA-50Ti (b); 30HA-70Ti (c).

To determine the wear resistance of the coatings, tribological tests were carried out according to the “ball-disk” scheme. The coefficient of friction of HA-Ti composite coatings with different content of hydroxyapatite is shown in Figure 9. The coefficient of friction of composite 30HA-70Ti coating was 0.510. An increase in the HA content to 70 wt. % leads to an increase in the coefficient of friction and the rate of wear of coatings. According to the obtained results of tribological testing of detonation 50HA-50Ti coating, low values of the friction coefficient of 0.352 and high wear resistance under sliding friction conditions were observed.

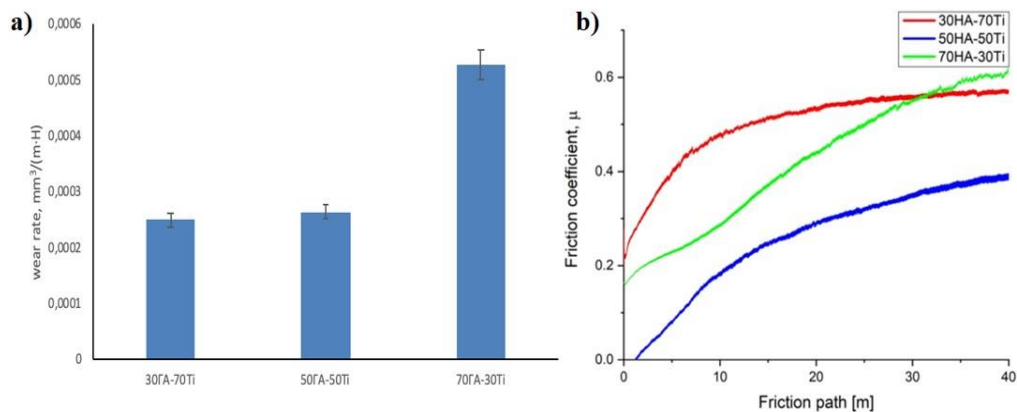


Figure 9. Intensity of wear (a) and coefficient of friction (b) of HA-Ti coatings (wt. %)

The study of the microstructure of the cross-section of the composite 50HA-50Ti coating showed the formation of a layered-porous structure with a thickness of 40-50 microns (Fig. 10 a). Elemental analysis data obtained from the coating layer correspond to the initial composition of the composite powder (Fig. 10 b).

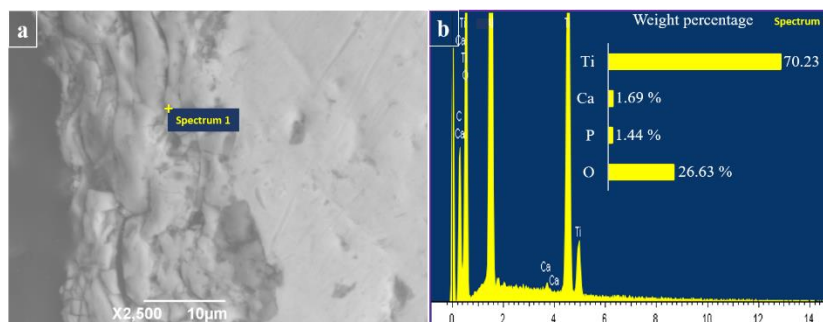


Figure 10. SEM image of a cross-section (a) and elemental analysis (b) of the composite 50HA-50Ti coating

### Conclusion

Crystalline composite coatings with a thickness of 40-50  $\mu\text{m}$  were obtained by the method of detonation spraying of 30HA-70Ti; 50HA-50Ti; 70HA-30Ti composites on the surface of Grade 2 titanium. Composite HA-Ti coatings have a layered porous structure. The results of X-ray phase analysis of detonation 50HA-50Ti and 70HA-30Ti coatings showed the formation of  $\alpha\text{-Ca}_3(\text{PO}_4)_2$  and TiO. Composite 30HA-70Ti coating is the closest in structure to stoichiometric crystalline HA ( $\text{Ca/P} = 1.67$ ). According to the results of Raman spectroscopy, the following structural features of the composite coating were revealed: with a decrease in the HA content, a decrease in the relative content of B-type carbonate ions in the structure of hydroxyapatite is observed, as well as a decrease in the content of the mineral phase in general. Based on the phase analysis and mechanical properties, the optimal content of the Ti additive was 50 wt. % for HA-Ti composite coatings sprayed with the CCDS2000 detonation complex used in experimental conditions.

### Acknowledgment

*This research was funded by the Science Committee of the Ministry of Education and Science of the Republic of Kazakhstan (Grant No. AP13068485).*

### References

- 1 Corpe, R.S., Young, T.R., Steflik, D.E., Whitehead, R.Y., Wilson, M.D., & Jaramillo, C. (2000). Correlative experimental animal and human clinical retrieval evaluations of hydroxyapatite (HA)-coated and non-coated implants in orthopaedics and dentistry. *Journal of Critical Reviews in Biomedical Engineering. Prefac*, 28, 395–398.
- 2 Cattini, A., Bellucci, D., Sola, A., Pawłowski, L., & Cannillo, V. (2013). Suspension plasma spraying of optimized functionally graded coatings of bioactive glass/hydroxyapatite. *Surface Coatings Technology*, 236, 118-126.
- 3 Rakhadilov, B.K., Baizhan, D.R., Sagdoldina, Zh.B., & Torebek, K. (2022). Research of regimes of applying coats by the method of plasma electrolytic oxidation on Ti-6Al-4V. *Bulletin of the university of Karaganda-Physics*, 1, 99–106.
- 4 Prosolov, K.A., Lastovka, V.V., Belyavskaya, O.A., Lychagin, D.V., Schmidt, J., & Sharkeev, Y.P. (2020). Tailoring the Surface Morphology and the Crystallinity State of Cu- and Zn-Substituted Hydroxyapatites on Ti and Mg-Based Alloys. *Materials*, 13 (19), 4449.
- 5 Rakhadilov, B., & Baizhan, D. (2021). Creation of Bioceramic Coatings on the Surface of Ti-6Al-4V Alloy by Plasma Electrolytic Oxidation Followed by Gas Detonation Spraying. *Coatings*, 11.
- 6 Vadiraj, A., & Kamaraj, M. (2007). Effect of surface treatments on fretting fatigue damage of biomedical titanium alloys. *Tribology International*, 40 (1). 82-88.
- 7 Dong, Z.L., Khor, K.A., Quek, C.H., White, T.J., & Cheang, P. (2003). TEM and STEM analysis on heat-treated and in vitro plasma-sprayed hydroxyapatite/Ti-6Al-4V composite coatings. *Biomaterials*, 24(1), 97-105.
- 8 Kang, A.S. (2020). Wear performance of hydroxyapatite coatings deposited on AISI 304L using detonation gun spray. *Materials Today: Proceedings*, 32(3), 304-310.
- 9 Ulianitsky, Yu.V., Dudina, D.V., Shtertser, A.A., & Smurov, I. (2019). Computer-Controlled Detonation Spraying: Flexible Control of the Coating Chemistry and Microstructure. *Metals*, 9(12), 1244.
- 10 Sagdoldina, Z., Rakhadilov, B., Skakov, M., & Stepanova, O. (2019). Structural evolution of ceramic coatings by mechanical alloying. *Materials testing*, 61, 304–308.
- 11 Savitzky, A. (1964). Smoothing and Differentiation of Data by Simplified Least Squares Procedures. *Analytical Chemistry*, 36(8), 1627-1639.
- 12 Oliver, W.C., & Pharr, G.M. (1992). An improved technique for determining hardness and elastic modulus using load and displacement sensing indentation experiments. *Journal of Materials Research*, 7(6), 1564-1583.
- 13 Fidancevska, E. (2007). Fabrication and characterization of porous bioceramic composites based on hydroxyapatite and titania. *Materials Chemistry and Physics*, 103(1), 95-100.
- 14 Yonggang, Y., Wolke, J.G.C., Yubao, L., & Jansen, J.A., The influence of discharge power and heat treatment on calcium phosphate coatings prepared by RF magnetron sputtering deposition, *Journal of Materials Science: Materials in Medicine*, 18, 1061-1069.
- 15 Baizhan, D.R., Rakhadilov, B.K., Zhurerova, L.G., & Torebek, K. (2022). Preparation of bio-ceramic composite coatings on Ti6Al4V titanium alloy by gas-detonation spraying. *Bulletin of the university of Karaganda-Physics*, 1, 89–98.
- 16 Rakhadilov, B., Kakimzhanov, D., Baizhan, D., Muslimanova, G., Pazylybek, S., & Zhurerova L. (2021). Comparative Study of Structures and Properties of Detonation Coatings with alpha-Al<sub>2</sub>O<sub>3</sub> and gamma-Al<sub>2</sub>O<sub>3</sub> Main Phases. *Coatings*, 11.
- 17 Timchenko, E.V., Timchenko, P.E., Taskina, L.A., Volova, L.T., Miljakova, M.N., & Maksimenko, N.A. (2015). Using Raman spectroscopy to estimate the demineralization of bone transplants during preparation. *J. Opt. Technol.*, 82 (3), 153-157.
- 18 Leyland, A., & Matthews, A. (2000). On the significance of the H/E ratio in wear control: a nanocomposite coating approach to optimised tribological behavior. *Wear*, 246 (1-2), 1-11.

19 Maksakova, O.V., Pogrebnyak, A.D., Yerbolatova, G., Beresnev, V.M., Kupchishin, A.I., & Baymoldanova, L.S. (2019). Triple sandwich design of multilayered (CrN/ZrN)/(Cr/Zr) hard coating with nanoscale architecture: microstructure and composition. *Materials Research Express*, 6 (10).

Ж.Б. Сағдолдина, Д.Р. Байжан, Б.К. Рахадиллов, Д.Б. Буйткенов,  
Н.Е. Бердімуратов, М.С. Жапарова

### Детонациялық бүрку әдісімен алынған НА/Ті композициялық жабындардың микроқұрылымы және механикалық қасиеттері

Мақалада гидроксипатит (ГА) және әртүрлі қатынастарда (мас. %): 30ГА-70Ті, 50ГА-50Ті, 70ГА-30Ті титан негізіндегі композициялық жабындардың құрылымы мен механикалық-трибологиялық қасиеттерінің нәтижелері келтірілген. Қалыңдығы 40-50 мкм композиттік жабындар детонациялық бүрку әдісімен ВТ1-0 (Grade 2) титаннан жасалған субстратқа алынды. Жабындардың микроқұрылымы мен фазалық құрамы сканерлеуші электронды микроскопия және рентгендік дифракция әдістерімен талданды. НА-Ті композиттік жабындарының бүрку механизмі де зерттелді. Зерттеу нәтижелері ГА-Ті қоспасынан ұнтақты детонациялық бүрку кезінде Са<sub>10</sub>(РО<sub>4</sub>)<sub>6</sub>(ОН)<sub>2</sub> гидроксипатит фазаларынан, трикальций фосфатынан, титаннан және титан оксидінен тұратын кеуекті жабындар түзілетінін көрсетті. Композиттегі гидроксипатит мөлшері азайған кезде құрылымдағы В типті карбонат иондарының салыстырмалы құрамы төмендейтіні, сондай-ақ жалпы минералды фазаның азаюы анықталды. 30НА-70Ті мас.% композициялық жабын құрылымы бойынша стехиометриялық кристалды НА-ға ең жақын (Са/Р = 1.67). 50 НА-50 Ті жабындарының арақатынасында тозуға төзімділіктің 1,5-2 есе артуы байқалады.

*Кілт сөздер:* гидроксипатит, титан, детонациялық бүрку, жабын, микроқұрылымы және фазалық құрамы, механикалық қасиеттері.

Ж.Б. Сағдолдина, Д.Р. Байжан, Б.К. Рахадиллов, Д.Б. Буйткенов,  
Н.Е. Бердімуратов, М.С. Жапарова

### Микроструктура и механические свойства композиционных покрытий НА/Ті, нанесенных методом детонационного напыления

В статье представлены результаты экспериментальных исследований структуры и механо-трибологических свойств композиционных покрытий на основе гидроксипатита (ГА) и титана в разных соотношениях (масс. %): 30ГА-70Ті, 50ГА-50Ті, 70ГА-30Ті. Композиционные покрытия толщиной 40-50 мкм были нанесены на подложку из титана марки ВТ-0 (Grade 2) методом детонационного напыления. Микроструктуру и фазовый состав напыленных покрытий анализировали методами сканирующей электронной микроскопии и рентгеновской дифракции. Также был исследован механизм напыления композитных покрытий НА-Ті. Результаты исследования показали, что при детонационном напылении порошка из смеси ГА-Ті формируются пористые покрытия, состоящие из фаз гидроксипатита Са<sub>10</sub>(РО<sub>4</sub>)<sub>6</sub>(ОН)<sub>2</sub>, трикальцийфосфата, титана и оксида титана. Было обнаружено, что при уменьшении содержания гидроксипатита в композите наблюдается снижение относительного содержания карбонат-ионов В-типа в структуре, а также уменьшение содержания минеральной фазы в целом. Композиционное покрытие 30ГА-70 Ті масс. %, наиболее близко по структуре к стехиометрическому кристаллическому ГА (Са/Р=1,67). При соотношениях покрытий 50ГА-50Ті масс. % наблюдается увеличение износостойкости в 1,5-2 раза.

*Ключевые слова:* гидроксипатит, титан, детонационное напыление, покрытие, микроструктуры и фазовый состав, механические свойства.